Dalton Transactions

Energetic Furazan-triazole Hybrid with Dinitromethyl and Nitramino Groups: Decreasing Sensitivity via the Formation of a Planar Anion

Journal:	*Dalton Transactions*
Manuscript ID	DT-ART-04-2019-001514.R1
Article Type:	Paper
Date Submitted by the Author:	30-Apr-2019
Complete List of Authors:	Shreeve, Jean'ne; University of Idaho, Department of Chemistry Tang, Yongxing; University of Idaho, Chemistry He, Chunlin; University of Idaho, Chemistry Imler, Gregory; US Naval Research Laboratory, Crystallography Parrish, Damon; Naval Research Laboratory,

Journal Name

ARTICLE

Energetic Furazan-triazole Hybrid with Dinitromethyl and Nitramino Groups: Decreasing Sensitivity via the Formation of a Planar Anion

Received 00th January 20xx,
Accepted 00th January 20xx

DOI: 10.1039/x0xx00000x

www.rsc.org/

Yongxing Tang,[a] Chunlin He,[ab] Gregory H. Imler,[c] Damon A. Parrish[c] and Jean'ne M. Shreeve*[a]

Energetic salts (**4**, **5** and **7**-**11**) of [3-(dinitromethanide)-1*H*-1,2,4-triazol-5-yl]-4-nitraminofurazanate and the azo compound (**15**) as well as its ammonium (**14**), hydrazinium (**16**) and hydroxylammonium (**17**) salts were synthesized and fully characterized. The structures of **5** and **15** were confirmed by single crystal X-ray diffraction analysis. The hydroxylammonium salt (**5**) has a high measured density (1.85 g cm^{-3}) and shows promising properties as a replacement for the traditional explosive (RDX). The anion is planar which suggests that a combination of two heterocylic five-membered rings with nitramino and dinitromethyl groups could open a new avenue to advanced energetic materials with high detonation performance and good sensitivities.

Introduction

Development of next generation energetic materials that could be used in practical military and civilian applications has aroused great interest in recent decades.[1] New energetic materials demand high performance, insensitivity and good thermal stability.[2] Therefore, understanding their structure-property relationships is very important in designing the ideal candidates for specific applications. Nitrogen-rich heterocyclic energetic compounds are generally accepted as having a skeleton which is important in assisting in the development of novel molecules. The introduction of different energetic groups modulates the properties of the target compounds.[3] Realization of high performance is the driving force in the search for new energetic materials for defense use and the source is most often nitro-containing moieties. However, the larger the number of nitro groups in a small single five-membered heterocyclic ring, the higher the sensitivity.[4] The effect of the presence of many explosophores can be dispersed over two or more nearly planar rings decreasing the nitro electron density through delocalization and thus concomitantly the sensitivity.

Dinitromethyl and nitramino groups are attractive explosophore groups, which exhibit good oxygen balance and can enhance compound density thus improving detonation performance.[5] Recently energetic derivatives of single triazole ring or furazan ring bearing nitramino and dinitromethyl moieties were reported and showed excellent detonation performance, but their high sensitivities would limit practical applications. (Fig. 1a, Fanion;[6] Fig.1b, Tanion[7]). The reasons might be: 1) the explosophore groups are highly concentrated on a single five-membered ring; or 2) the dinitromethyl group is twisted out of the plane of the skeleton. However, the salts that were recently reported based on 4-nitramino-3-(5-dinitromethyl-1,2,4-oxadiazolyl)-furazan[8] exhibit good detonation performance and acceptable sensitivities. Examination of the crystal structure shows that the anion is planar enhancing π-π interactions which can play an important role in decreasing sensitivity.

With our continuing interest in pursuing such suitable candidates, we report several energetic salts based on 3-(3-dinitromethanide-1*H*-1,2,4-triazol-5-yl)-4-nitraminofurazanate involving furazan and triazole rings as well as nitramino and dinitromethyl substituents (Scheme 1). The crystal structure of **5** confirms the presence of a planar anion (FTanion) which gives rise to lower sensitivities relative to the energetic salts based on

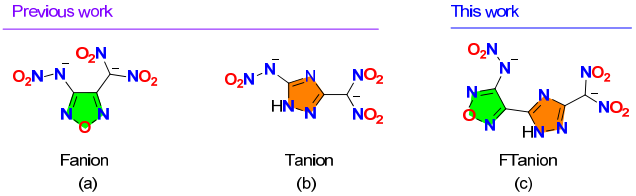

Fig. 1 Skeletons with nitramino and dinitromethyl substituent groups

[a] Department of Chemistry, University of Idaho, Moscow, Idaho, 83844-2343 USA. Fax: (+1) 208-885-9146 E-mail: jshreeve@uidaho.edu
[b] School of Materials Science & Engineering, Beijing Institute of Technology, Beijing, China
[c] Naval Research Laboratory, 4555 Overlook Avenue, Washington, D.C. 20375 USA
† Footnotes relating to the title and/or authors should appear here.
Electronic Supplementary Information (ESI) available: Includes theoretical calculation, crystallographic data (CCDC: 1891124 and 1891126). See DOI: 10.1039/x0xx00000x

Fanion and Tanion (Fig. 1). In addition, the azo bridged neutral compound **15** and its ammonium (**14**), hydrazinium (**16**) and hydroxylammonium (**17**) salts were also prepared.

Results and discussion

Synthesis

4-Amino-1,2,5-oxadiazole-3-carboximihydrazide[9] (**1**) when reacted with ethyl 3-ethoxy-3-iminopropanoate hydrochloride in the presence of boron trifluoride diethyl etherate gave **2** (Scheme 1). The nitration of **2** with a mixture of 100% nitric acid and concentrated sulfuric acid gave the intermediate **3**, which was extracted from the acid solution and treated without purification with aqueous methanolic ammonia (2 N). A yellow powder (**4**) precipitated from the solution and was isolated by filtration. Similarly, the hydroxylammonium salt (**5**) was obtained by reacting **3** with 50% hydroxylamine. The other salts (**7**–**12**) were synthesized readily from the silver salt (**6**) and the corresponding hydrochloride salts.

Compound **12** resulted from the oxidation of **2** using potassium permanganate ($KMnO_4$) in acidic solution (Scheme 2). Compound **12** with a mixture of concentrated sulfuric acid and 100% nitric acid leads to the formation of the dinitro substituted product **13**, which was decarboxylated by using methanolic ammonia to give **14**. Acidification of **14** with concentrated HCl in acetone resulted in the neutral compound **15**. The hydrazinium (**16**) and hydroxylammonium (**17**) salts were synthesized readily by reacting **15** with monohydrazine and hydroxylamine, respectively.

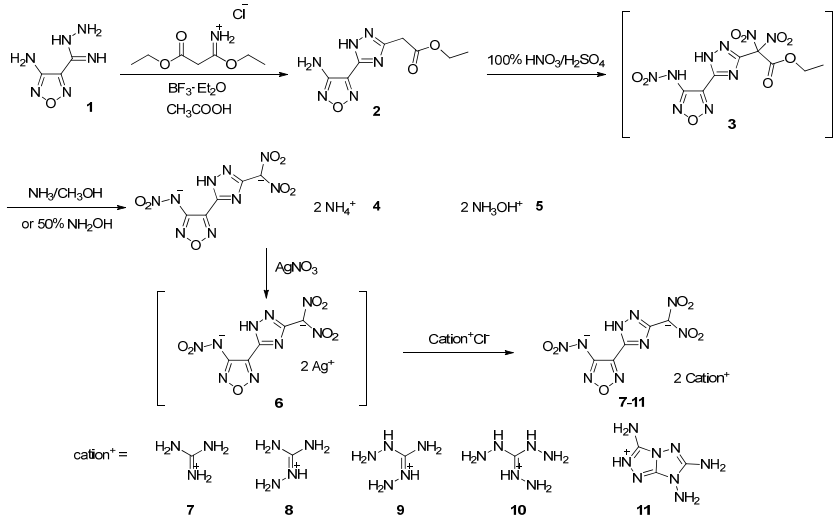

Scheme 1 Synthesis of energetic salts **4**, **5** and **7**-**11.**

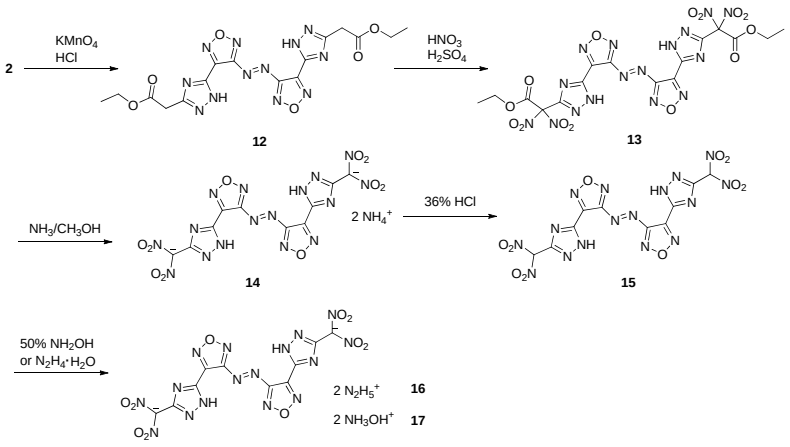

Scheme 2 Synthesis of **15** and its energetic salts (**14**, **16** and **17**)

Single-crystal X-ray structure analysis

Compound **5** crystallizes from a mixture of methanol and water in the triclinic space group P-1 with a high density of 1.887 g cm^{-3} (150 K) with two formula moieties in a unit cell. The molecular structure is shown in Fig. 2a. The dinitromethyl group, triazole ring, furazan ring and nitramino group are nearly coplanar. The torsion angle of N(3)-N(4)-C(5)-N(6) is 1.5(6)°, while those of C(5)-C(9)-C(10)-N(11) and N(14)-C(13)-C(15)-N(16) are 1.8(6)° and 179.6(3)°, respectively. There are many hydrogen bonds as shown in the packing diagram of **5** (Fig. 2b). The planar anion in **5** resulted in the formation of face-to-face π-π interactions with a distance of 3.04 Å. In the layer structure (Fig. 2c), several intermolecular hydrogen bonds involving N–H•••O, O–H•••N were found. Further details are available in the ESI.

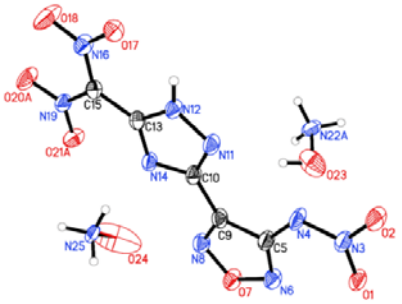

(a)

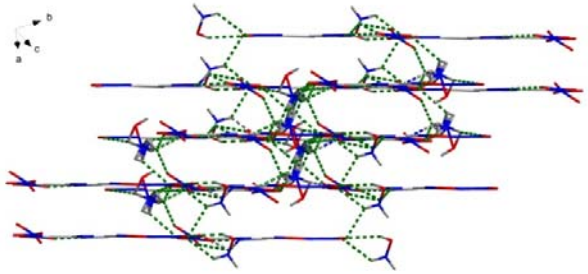

(b)

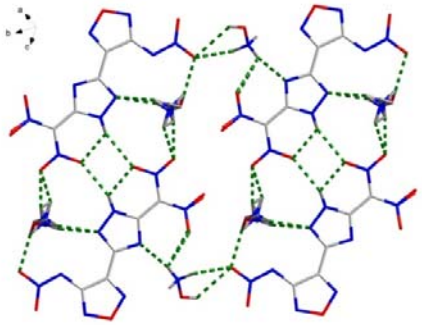

(c)

Fig. 2 (a) The molecular structure of **5**; (b) Packing diagram of **5**, green dashed lines represent hydrogen bonds; (c) Hydrogen bonding interactions in a plane of **5** along *b* axis

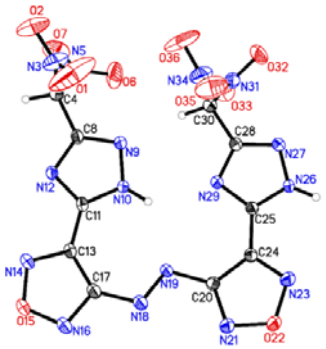

(a)

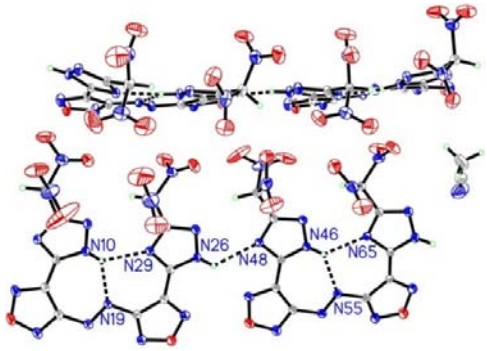

(b)

Fig. 3 (a) The molecular structure of **15**; The solvent acetonitrile is omitted for clarity; (b) Hydrogen bonding interactions in **15**.

Suitable crystals (**15**) for single-crystal X-ray diffraction were obtained by slow evaporation in acetonitrile solution. It crystallizes in the monoclinic space group $P2_1/n$ with sixteen molecules in the unit cell. The crystal structure is shown in Fig. 3a. There are four kinds of molecules in the unit cell with essentially identical bond lengths and bond angles. The details are given in the ESI. The azo bridge appears in the trans conformation in which C17-N18-N19-C20 torsion angle is -177.63° and the bond length of N18-N19 is 1.258 Å. The two triazole rings connected to the azo furazan moiety face in the same direction; thus they form intramolecular hydrogen bonds (N10–H10···N19, N10–H10···N29, N46–H46···N55 and N46–H46···N65) and intermolecular hydrogen bond (N26–H26···N48) (Fig. 3b). In addition, due to steric hindrance, the two triazole rings are slightly different with torsion angles of N(23)-C(24)-C(25)-N(29) = -179.5(2)° and N(12)-C(11)-C(13)-C(17) = -168.6(2)°. The nitro groups are twisted out of the planes of the connected triazole rings.

Physiochemical properties and energetic performances

Physical and some key energetic properties of these synthesized compounds, such as decomposition temperatures, densities, heats of formation, detonation properties and sensitivities, are summarized in Table 1. The thermal stability was determined by differential scanning calorimetric (DSC) measurements at a heating rate of 5 °C min^{-1}. The onset decomposition temperatures ranged from 146 °C to 197 °C for the energetic salts (**4**, **5** and **7**-**11)** based on

Table 1. Physical and detonation properties of **4, 5, 7-11, 14-17** compared with TNT and RDX.

Compounds	T_d[a] [°C]	ρ[b] [g cm^{-3}]	$\Delta_f H$[c] [kJ mol^{-1}/kJ g^{-1}]	vD[d] [m s^{-1}]	P[e] [Gpa]	IS[f] [J]	FS[g] [N]
4	167	1.78	267.7/0.80	8655	31.3	23	>360
5	190	1.85(1.863)[i]	156.1/0.43	8897	35.8	20	>360
7	146	1.65	185.2/0.44	7855	22.7	30	>360
8	197	1.72	396.5/0.88	8385	26.6	25	>360
9	172	1.68	636.1/1.33	8412	26.5	25	>360
10	145	1.74	850.4/1.67	8868	30.1	30	>360
11	188	1.73	1338.6/2.20	8358	26.8	32	>360
14	165	1.63	511.7/0.88	7938	24.7	18	240
15	120	1.76(1.731)[i]	904.9/1.78	8363	29.2	5	80
16	169	1.72	1256.9/2.20	8480	29.7	8	120
17	105	1.75	1050.3/1.83	8559	31.5	10	120
TNT	300	1.65	-59.3/-0.26	6881	19.5	15	353
RDX	204	1.80	70.3/0.32	8795	34.9	7.4	120

[a] Thermal decomposition temperature (onset) under nitrogen gas (DSC, 5 °C/min). [b] Measured densities - gas pycnometer at room temperature. [c] Calculated heat of formation. [d] Calculated detonation velocity. [e] Calculated detonation pressure. [f] Impact sensitivity. [g] Friction sensitivity. [i] The crystal densities at room temperature (There is CH_3CN solvent in **15**)

[3-(dinitromethanide)-1*H*-1,2,4-triazol-5-yl]-4-nitraminofurazanate. The azo bridged dinitromethyl compound (**15**) decomposes at 120 °C, while the ammonium (**14**), hydrazinium (**16**) and hydroxylammonium (**17**) salts based on **15** decompose at 165 °C, 169 °C and 105 °C, respectively. Densities were measured using a gas pycnometer. All of them are moderately dense with **5** being the densest at 1.85 g cm^{-3}. The heats of formation were calculated using the Gaussian 03 suite of programs[10] on the basis of the Born-Haber energy cycle and isodesmic reactions (ESI). These new compounds exhibit positive heats of formation, e.g., **11**, **16** and **17** have heats of formation > 1000 kJ mol^{-1}. With the measured densities and calculated heats of formation in hand, the two important detonation parameters, viz., detonation velocity and detonation pressure, were calculated by using EXPLO 5 v6.01 code.[11] The detonation velocities lie in the range between 7855 m s^{-1} (**7**) and 8897 m s^{-1} (**5**), which are much higher than that of TNT (6881 m s^{-1}). The hydroxylammonium (**5**) and triaminoguanidinium (**10**) salts have similar detonation velocities (**5**: 8897 m s^{-1}; **10**: 8868 m s^{-1}), which are superior to RDX (8795 m s^{-1}). Detonation pressures are in the range of 22.7 GPa (**7**) to 35.8 GPa (**5**).

Considering safety applications, the impact and friction sensitivities were measured according to standard BAM techniques.[12] As can been seen in Table 1, the energetic salts (**4**, **5**, **7**-**11**) based on the FTanion are less impact sensitive (at 20-32 J) than TNT and RDX. The friction sensitivities are greater than 360 N, showing that they are insensitive to friction. In comparison, the salts (**4**, **5**, **7**-**11**) based on the furazan-triazole core are also less sensitive than those based on the dinitromethyl-nitramino-substituted mono-ring skeleton (either furazan or triazole, Fig. 1a and 1b). The dinitromethyl substituted azo bridged neutral compound **15** and its salts (**14**, **16** and **17**) are more sensitive than the salts based on FTanion (Fig. 1c), which might be caused by the highly distorted structures of **14**-**17**.

To gain further insight into the relationship between sensitivity and structure, the crystal structures of those anions are shown in Figure 4. In the structures of the 3-nitramino-4-dinitromethyl-furazanate (Fig. 4a, Fanion) and 3-nitramino-5-dinitromethyl-1,2,4-triazolate (Fig. 4b, Tanion), the dinitromethyl groups are twisted out of the plane of the central ring. However, when the triazole and furazan rings are combined in the same molecule, the dinitromethyl group substituents are nearly coplanar with the rings (Fig. 4c,

FTanion). Previous studies show that a planar structure reduces "hotspots" caused by sliding arising from an external mechanical force.[14] Therefore, in comparison with the highly

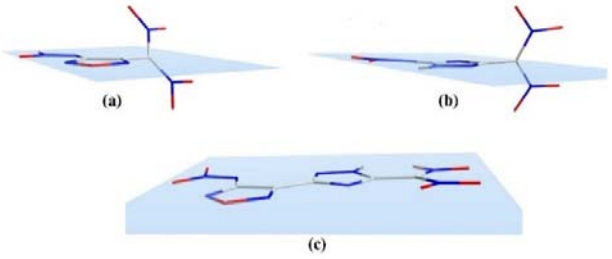

Fig. 4 The crystal structures of 3-nitramino-4-dinitromethyl-furazanate (a, Fanion) and 3-nitramino-5-dinitromethyl-1,2,4-triazolate (b, Tanion), [3-(dinitromethanide)-1*H*-1,2,4-triazol-5-yl]-4-nitraminofurazanate (c, FTanion)

distorted structures of Fanion and Tanion, planar molecules or anions (FTanion) lead to lower sensitivities. This is supported by the experimental data.

The electrostatic potential (ESP) on the ionic vdW surface was also employed to study impact sensitivities.[13] The most negative potentials of Fanion, Tanion and FTanion were calculated by Multiwfn[15] and are given shown in Table 2. As can been seen, the values of ESP in the FTanion are much lower than those in Fanion or Tanion, supporting the observations that the energetic salts based on FTainon are less sensitive than those based on Fanion or Tanion.

Table 2. Most negative electrostatic potentials on the 0.001 au surfaces of Fanion, Tanion, and FTanion

Anion	Most negative electrostatic potentials, kcal/mol
Fanion (Fig. 4a)	-194, -182, -179, -179, -176, -175, -170
Tanion (Fig. 4b)	-179, -178, -178, -175, -174, -174, -169, -168, -167
FTanion (Fig. 4c)	-183, -177, -170, -165, -154, -150, -146

Conclusions

In conclusion, energetic salts (**4**, **5** and **7**-**11**) of [3-(dinitromethanide)-1*H*-1,2,4-triazol-5-yl]-4-nitraminofuraza-nate and the azo compound (**15**) as well as its ammonium (**14**), hydroxylammonium (**16**) and hydrazinium (**17**) salts were synthesized and fully characterized. The structures of **5** and **15** were also confirmed by single crystal X-ray diffraction analysis. The energetic salt **5** has a high density of 1.85 g cm^{-3} and promising detonation properties (*v*D: 8897 ms^{-1} *P*: 35.8 GPa) with acceptable sensitivities which are comparable to those of the high explosive RDX. Enlarging the skeleton does offer an efficient way to decrease sensitivity relative to most highly nitro-functionalized salts based on mono nitrogen-rich rings which are sensitive.

Experimental Section

Caution! The compounds in this work are potential energetic materials that could explode under certain conditions (e.g., impact, friction or electric discharge). Appropriate safety precautions, such as the use of shields in a fume hood and personal protection equipment (safety glasses, face shields, ear plugs, as well as gloves) should be taken all the time when handling these materials.

General methods

All reagents were purchased from AKSci or Alfa Aesar in analytical grade and were used as supplied. ^{1}H, ^{13}C, and ^{15}N NMR spectra were recorded on a 300 MHz (Bruker AVANCE 300) or 500 MHz (Bruker AVANCE 500) nuclear magnetic resonance spectrometer. Chemical shifts for ^{1}H and ^{13}C spectra are given with respect to external $(CH_3)_4Si$ (^{1}H and ^{13}C). [D_6]DMSO was used as a locking solvent unless otherwise stated. IR spectra were recorded using KBr pellets with a FT-IR spectrometer (Thermo Nicolet AVATAR 370). Density was determined at room temperature by employing a Micromeritics AccuPyc II 1340 gas pycnometer. Decomposition (onset) points were recorded with a purge of dry nitrogen gas and a heating rate of 5 °C min^{-1} on a differential scanning calorimeter (DSC, TA Instruments Q2000). Elemental analyses (C, H, N) were performed on a Vario Micro cube Elementar Analyser. Impact and friction sensitivity measurements were made using a standard BAM Fallhammer and a BAM friction tester.

Computational Methods

The gas phase enthalpies of formation were calculated based on isodesmic reactions (Scheme S1, ESI). The enthalpy of reaction is obtained by combining the MP2/6–311++G** energy difference for the reactions, the scaled zero point energies (ZPE), values of thermal correction (HT), and other thermal factors. The solid state heats of formation were calculated with Trouton's rule according to equation 1 (*T* represents either the melting point or the decomposition temperature when no melting occurs prior to decomposition).[16]

$$\Delta H_{sub} = 188 / Jmol^{-1}K^{-1} \times T \quad (1)$$

For energetic salts, the solid-phase enthalpy of formation is obtained using a Born−Haber energy cycle.[17] For the compound which is hydrate (**14**·$2H_2O$), the solid-phase enthalpy of formation is obtained by adding the gas phase heat of formation of anhydrous compound to that of water (-241.8 kJ mol^{-1}).[18]

X-Ray crystallography data

A clear yellow plate crystal (**5**) of dimensions 0.170 × 0.077 × 0.010 mm^3, or a clear yellow plate crystal (**15**) of dimensions 0.340 × 0.212 × 0.106 mm^3 was mounted on a MiteGen MicroMesh using a small amount of Cargille immersion oil. Data were collected on a Bruker three-circle platform diffractometer equipped with a SMART APEX II CCD detector. The crystals were irradiated using graphite monochromated MoK_α radiation (λ = 0.71073 Å). An Oxford Cobra low temperature device was used to keep the crystals at a constant 150(2)K during data collection.

Data collection was performed and the unit cell was initially refined using *APEX3* [v2015.5-2].[19] Data reduction was performed using *SAINT* [v8.34A][20] and *XPREP* [v2014/2].[21] Corrections were applied for Lorentz, polarization, and absorption effects using *SADABS* [v2014/2].[22] The structure was solved and refined with the aid of the program SHELXL-

2014/7.[23] The full-matrix least-squares refinement on F^2 included atomic coordinates and anisotropic thermal parameters for all non-H atoms. The H atoms were included using a riding model.

In the crystal structure of **5**, there is a significant disorder in the cation channels. One of the hydroxylammonium cations has only partial occupancy and is partially replaced by an ammonium cation (NH_4: NH_3OH = 0.82:0.18). One of the nitro groups is disordered over two positions and has been modeled with an 85:15 ratio.

Synthesis of ethyl 2-[5-(4-amino-1,2,5-oxadiazol-3-yl)-1*H*-1,2,4-triazol-3-yl)]acetate (2)

A suspension of 4-amino-1,2,5-oxadiazole-3-carboximihydrazide (**1**, 2.84 g, 20 mmol),[9] ethyl 3-ethoxy-3-iminopropanoate hydrochloride (4.3 g, 22 mmol) and 20 drops of boron trifluoride diethyl etherate in acetic acid (50 mL) was heated to 50 °C for 3 h. Then the reaction mixture was heated under reflux for 18 h. After the solution cooled to ambient temperature, the insoluble solids were removed by filtration, and the filtrate was concentrated under vacuum in a rotary evaporator. The residue was suspended in water (200 mL) and neutralized with solid sodium bicarbonate to pH ~ 5-6. The pale-white solids were collected by filtration and dried in air to give product **2** (3.57 g, 75% yield). T_m: 165 °C. $T_{d(onset)}$: 270 °C. ^{1}H NMR: δ 14.63 (br), 6.41 (s, 2H), 4.13 (q, 2H), 4.05 (s, 2H), 1.21 (t, 2H) ppm. ^{13}C NMR: δ 167.9, 155.2, 152.1, 149.3, 139.1, 61.1, 32.3, 13.9 ppm. IR (KBr): $\tilde{\nu}$ 3508, 3467, 3405, 3168, 1742, 1730, 1705, 1625, 1561, 1549, 1464, 1396, 1370, 1323, 1220, 1183, 1097, 1063, 1026, 1008, 981, 899, 874, 862, 809, 767, 734, 663 cm^{-1}. Elemental analysis for $C_8H_{10}N_6O_3$ (238.20): Calcd C 40.34, H 4.23, N 35.28 %. Found: C 40.64, H 4.78, N 35.03 %.

Synthesis of 4

Compound **2** (1.0 g, 4.2 mmol) was added slowly to a cooled and well-stirred mixture of concentrated sulfuric acid (10 mL) and 100% nitric acid (4 mL) at 0 °C. The temperature was allowed to warm slowly to room temperature over a period of 1 h, and the mixture was stirred for an additional 24 h. The solution was poured into ice water (100 g) and extracted with diethyl ether (20 mL × 3). The combined organic phases were washed with brine (20 mL × 2) and dried over magnesium sulfate and filtered. The solvent was evaporated at ambient temperature under vacuum to give a light yellow oil to which ethanol (15 mL) was added. The solution was stirred and methanolic ammonia (2 M, 2 mL) was added. After 2 h, the yellow precipitate was collected by filtration, washed with ethanol (10 mL), and diethyl ether (10 mL) to give **4** (0.89 g, yield: 63%). Yellow solids. $T_{d(onset)}$: 167 °C. ^{1}H NMR: δ 7.94 (br) ppm. ^{13}C NMR: δ 157.5, 150.3, 149.3, 144.9, 124.2 ppm. IR (KBr): $\tilde{\nu}$ 3220, 1536, 1507, 1430, 1405, 1301, 1095, 1031, 1011, 98, 828, 745 cm^{-1}. Elemental analysis for $C_5H_9N_{11}O_7$ (335.19): Calcd C 17.92, H 2.71, N 45.97 %. Found: C 18.22, H 2.84, N 43.36 %.

Synthesis of 5

Compound **2** (1.0 g, 4.2 mmol) was added slowly to a cooled and well-stirred mixture of concerntrated sulfuric acid (10 mL) and 100% nitric acid (4 mL) at 0 °C. The temperature was allowed to warm slowly to room temperature over a period of 1 h, and the mixture was stirred for an additional 24 h. The solution was poured into ice water (100 g) and extracted with diethyl ether (20 mL × 3). The combined organic phases were washed with brine (20 mL × 2) and dried over magnesium sulfate and filtered. The solvent was evaporated at ambient temperature under vacuum to give a light yellow oil to which ethanol (15 mL) was added. The solution was stirred and 50% hydroxylamine (10 mmol, 0.66 g) was added. After 2 h, the yellow precipitate was collected by filtration, washed with ethanol (10 mL), and diethyl ether (10 mL) to give **5** (0.69 g, yield: 45%). Yellow solid. $T_{d(onset)}$: 190 °C. ^{1}H NMR: δ 10.09 (br) ppm. ^{13}C NMR: δ 153.1, 150.0, 149.2, 145.5, 123.7 ppm. IR (KBr): $\tilde{\nu}$ 3149, 1608, 1518, 1471, 1438, 1397, 1240, 1178, 1137, 1089, 1004, 987, 828, 768, 746, 657, 538 cm^{-1}. Elemental analysis for $C_5H_9N_{11}O_9$ (367.19): Calcd C 16.35, H 2.47, N 41.96 %. Found: C 17.06, H 2.21, N 41.28 %.

General procedure for the synthesis of 7-11

The ammonium salt **4** (0.67 g, 2.0 mmol) was dissolved in water (30 mL). Silver nitrate (0.75 g, 4.4 mmol) was added. The reaction mixture was stirred for 2 h at room temperature. Silver salt **6** was obtained by filtration and washed with water (30 mL). Then **6** was suspended in water (50 mL), and two equivalents of the corresponding hydrochloride salt was added. The temperature of the reaction mixture was increased to 60 °C and it was stirred for 4 h. After removing the insoluble solids, the filtrate was concentrated to give the final products (**7–11**). Final purification resulted after recrystallization from hot water.

7 (0.71 g, 85%): Yellow solid. $T_{d(onset)}$: 146 °C. ^{1}H NMR: δ 6.92 (s) ppm. ^{13}C NMR: δ 157.9, 157.6, 150.4, 149.3, 145.1, 124.1 ppm. IR (KBr): $\tilde{\nu}$ 3427, 3431, 3275, 3192, 1652, 1567, 1497, 1481, 1425, 1383, 1323, 1300, 1229, 1182, 1139, 1033, 1015, 991, 929, 841, 769, 744 cm^{-1}. Elemental analysis for $C_7H_{13}N_{15}O_7$ (419.27): Calcd C 20.05, H 3.13, N 50.11 %. Found: C 19.95, H 3.11, N 50.16 %.

8 (0.79 g, 88%): Yellow solid. $T_{d(onset)}$: 197 °C. ^{1}H NMR: δ 8.83 (s, 1H), 7.85 (s, 4H), 4.68 (s, 2H) ppm. ^{13}C NMR: δ 158.8, 157.6, 150.3, 149.4, 145.1, 124.2 ppm. IR (KBr): $\tilde{\nu}$ 3426, 3346, 1680, 1554, 1509, 1432, 1406, 1297, 1226, 1190, 1124, 1085, 1033, 987, 944, 882, 830, 776, 769, 737 cm^{-1}. Elemental analysis for $C_7H_{15}N_{17}O_7$ (449.30): Calcd C 18.71, H 3.37, N 53.00 %. Found: C 18.82, H 3.25, N 53.24 %.

9 (0.77 g, 80%): Yellow solid. $T_{d(onset)}$: 172 °C. ^{1}H NMR: δ 8.53 (s, 2H), 7.19 (s, 2H), 4.58 (s, 4H) ppm. ^{13}C NMR: δ 159.7, 157.6, 150.3, 149.2, 145.0, 124.1 ppm. IR (KBr): $\tilde{\nu}$ 3425, 3137, 1689, 1548, 1534, 1495, 1428, 1394, 1296, 1227, 1179, 1132, 1102, 1030, 1007, 986, 916, 829, 769, 744, 715, 672, 597 cm^{-1}. Elemental analysis for $C_7H_{17}N_{19}O_7$ (479.33): Calcd C 17.54, H 3.57, N 55.52 %. Found: C 17.62, H 3.62, N 55.86 %.

10 (0.88 g, 86%): Yellow solid. $T_{d(onset)}$: 145 °C. ^{1}H NMR: δ 8.56 (s, 3H), 4.36 (s, 6H) ppm. ^{13}C NMR: δ 159.0, 157.3, 151.0, 148.7, 145.0, 124.0 ppm. IR (KBr): $\tilde{\nu}$ 3479, 3213, 1689, 1548, 1501,

1429, 1401, 1306, 1234, 1184, 1130, 1033, 984, 878, 825, 768, 738, 639, 557 cm^{-1}. Elemental analysis for $C_7H_{19}N_{21}O_7$ (509.36): Calcd C 16.51, H 3.76, N 57.75 %. Found: C 16.64, H 3.78, N 58.03 %.

11 (0.98 g, 80%) : Yellow solid. $T_{d(onset)}$: 188 °C. ^{1}H NMR: δ 8.16 (s, 2H), 7.21 (s, 2H), 5.76 (s, 2H) ppm. ^{13}C NMR: δ 160.1, 1575, 151.0, 148.7, 147.4, 145.4, 141.1, 123.9 ppm. IR (KBr): $\tilde{\nu}$ 3175, 3157, 3140, 1662, 1547, 1503, 1400, 1302, 1135, 1107, 984, 828, 769, 769, 742, 566 cm^{-1}. Elemental analysis for $C_{11}H_{15}N_{25}O_7$ (609.40): Calcd C 21.68, H 2.48, N 57.46 %. Found: C 21.54, H 2.32, N 56.92 %.

Synthesis of 12

Compound **2** (2.38 g, 10.0 mmol) was dissolved in concentrated HCl (20 mL) combined with water (40 mL), and the solution was cooled to < 10 °C in an ice bath. Then potassium permanganate (1.60 g, 10.0 mmol) suspended in a minimum amount of water was added dropwise to the reaction mixture while maintaining the reaction temperature < 10 °C. The solution was warmed to room temperature and stirred for 24 h. Dilute hydrogen peroxide (5%) was added until the solution became colorless. The precipitate was collected by filtration, washed with water (200 mL) and dried to give **12** (1.33 g, 56%). Yellow solid. $T_{d(onset)}$: 194 °C. ^{1}H NMR: δ 14.67 (s, 2H), 4.12 (q, 4H), 4.03 (s, 4H), 1.18 (t, 6H) ppm. ^{13}C NMR: δ 167.8, 161.8, 152.0, 148.9, 144.3, 61.1, 40.0, 13.9 ppm. IR (KBr): $\tilde{\nu}$ 3132, 2991, 1727, 1556, 1497, 1476, 1439, 1373, 1336, 1299, 1270, 1215, 1138, 1059, 1032, 990, 933, 886, 844 cm^{-1}. Elemental analysis for $C_{16}H_{16}N_{12}O_6$ (472.38): Calcd C 40.68, H 3.41, N 35.58 %. Found: C 40.38, H 3.34, N 35.41 %.

Synthesis of 13·H_2O

Compound **12** (0.52 g, 1.1 mmol) was added slowly to a cooled and well-stirred mixture of concentrated sulfuric acid (10 mL) and 100% nitric acid (3 mL) at 0 °C. The temperature was allowed to warm slowly to room temperature over a period of 1 h, and the mixture was stirred for an additional 24 h. The solution was poured into ice water (100 g) and the yellow precipitate was collected by filtration, washed with water (30 mL × 2) to give **13·H_2O** (0.50 g, yield: 68%).
Yellow solid. $T_{d(onset)}$: 190 °C. ^{1}H NMR: δ 4.54 (q, 4H), 1.29 (t, 6H) ppm. ^{13}C NMR: δ 161.8, 156.0, 151.3, 144.7, 141.2, 113.4, 66.7, 13.3 ppm. IR (KBr): $\tilde{\nu}$ 3182, 3089, 2974, 1756, 1662, 1583, 1501, 1456, 1437, 1399, 1185, 1038, 996, 924, 883, 816, 753, 692 cm^{-1}. Elemental analysis for $C_{16}H_{14}N_{16}O_{15}$ (670.38): Calcd C 28.67, H 2.10, N 33.43 %. Found: C 28.23, H 1.76, N 33.58 %.

Synthesis of 14·2H_2O

Methanolic ammonia (4 mL, 2.0 mol L^{-1}) was added to a suspension of **13** (0.34 g, 0.50 mmol) in ethanol (20 mL). The reaction mixture was stirred for 6 h at room temperature. The precipitate (**14**, 0.27 g, yield 94%) was collected by filtration, washed with ethanol (10 mL) and diethyl ether (10 mL). Yellow solid. $T_{d(onset)}$: 165 °C. ^{1}H NMR: δ 7.12 (br) ppm. ^{13}C NMR: δ 156.5, 152.6, 150.1, 139.8, 126.0 ppm. IR (KBr): $\tilde{\nu}$ 1636, 1584, 1529, 1503, 1440, 1325, 1245, 1195, 1081, 1035, 1007, 986, 925, 880, 861, 776, 743, 698, 617, 607 cm^{-1}. Elemental analysis for $C_{10}H_{14}N_{18}O_{12}$ (578.33): Calcd C 20.77, H 2.44, N 43.59 %. Found: C 20.56, H 2.66, N 43.05 %.

Synthesis of 15

Compound **14** (0.29 g, 0.50 mmol) was suspended in acetone (20 mL) at 25 °C. Concentrated HCl (0.5 mL) was added to the suspension. After stirring for 1 h, the white solid was separated by filtration. The filtrate was dried over magnesium sulfate and the solvent was removed. The remaining residue was solidified by adding dichloromethane (5 mL). The precipitate (**15**) was filtered and dried in air. The pure sample of **9** (0.20 g, 80%) was obtained as a yellow solid. $T_{d(onset)}$: 120 °C. ^{1}H NMR(CD_3CN): δ 8.24 (s, 2H) ppm. ^{13}C NMR (CD_3CN): δ 162.9, 153.1, 145.5, 141.4, 106.3 ppm. IR (KBr): $\tilde{\nu}$ 1577, 1445, 1400, 1328, 1239, 1192, 1145, 1059, 995, 873, 815, 785, 718 cm^{-1}. Elemental analysis for $C_{10}H_4N_{16}O_{10}$ (508.24): Calcd C 23.63, H 0.79, N 44.09 %. Found: C 23.95, H 1.13, N 44.83 %.

Synthesis of 16

Compound **15** (0.25 g, 0.50 mmol) was dissolved in ethanol (15 mL) at 25 °C. Then hydrazine monohydrate (0.10 g, 2.0 mmol) in ethanol (5 mL) was added slowly. After stirring for 1 h, the yellow solid was collected by filtration and dried in air to give **16** (0.26 g, 90%). $T_{d(onset)}$: 169 °C. ^{1}H NMR: δ 10.31 (br) ppm. ^{13}C NMR: δ 156.4, 152.5, 150.1, 139.9, 125.9 ppm. IR (KBr): $\tilde{\nu}$ 1608, 1570, 1518, 1430, 1394, 1224, 1172, 1123, 999, 986, 953, 871, 823, 783, 764, 750, 596 cm^{-1}. Elemental analysis for $C_{10}H_{12}N_{20}O_{10}$ (572.33): Calcd C 20.99, H 2.11, N 48.95 %. Found: C 21.23, H 2.45, N 50.12 %.

Synthesis of 17

Compound **15** (0.25 g, 0.50 mmol) was dissolved in ethanol (15 mL) at 25 °C. Then 50% hydroxylamine solution (0.13 g, 2.0 mmol) in ethanol (5 mL) was added slowly. After stirring for 1 h, the yellow solid was collected by filtration and dried in air to give **17** (0.23 g, 80%). $T_{d(onset)}$: 105 °C. ^{1}H NMR: δ 5.72 (br) ppm. ^{13}C NMR: δ 156.5, 152.6, 150.1, 139.8, 126.0 ppm. IR (KBr): $\tilde{\nu}$ 1624, 1533, 1484, 1400, 1214, 1132, 1099, 1028, 1006, 985, 883, 826, 764, 748, 659 cm^{-1}. Elemental analysis for $C_{10}H_{10}N_{18}O_{12}$ (574.30): Calcd C 20.91, H 1.76, N 43.90 %. Found: C 21.03, H 1.87, N 44.62 %.

Conflicts of interest

There are no conflicts to declare.

Acknowledgements

This work was supported by the Office of Naval Research (N00014-16-1-2089) and the Defense Threat Reduction Agency (HDTRA 1-15-1-0028). We are also grateful to the M. J. Murdock Charitable Trust, Reference No.: 2014120: MNL:11/20/2014 for funds supporting the purchase of a 500 MHz NMR spectrometer.

Notes and references

1 (*a*) J. P. Agrawal and R. Hodgson, *Organic Chemistry of Explosives*, John Wiley & Sons, 2007; (*b*) T. M. Klapötke, *Chemistry of High-energy Materials*, 4th ed.; De Gruyter: Berlin, 2017; (*c*) P. Wang, Y. Xu, Q. Lin and M. Lu, *Chem. Soc. Rev.*, 2018, **47**, 7522; (*d*) Y. Xu, Q. Wang, C. Shen, Q. Lin, P. Wang and M. Lu, *Nature*, 2017, **549**, 78.

2 (*a*) B. C. Tappan, M. H. Huynh, M. A. Hiskey, D. E. Chavez, E. P. Luther, J. T. Mang and S. F. Son, *J. Am. Chem. Soc.*, 2006, **128**, 6589; (*b*) M. C. Schulze, B. L. Scott and D. E. Chavez, *J. Mater. Chem. A*, 2015, **3**, 17963; (*c*) I. L. Dalinger, O. V. Serushkina, N. V. Muravyev, D. B. Meerov, E. A. Miroshnichenko, T. S. Kon'kova, K. Y. Suponitsky, M. V. Vener and A. B. Sheremetev, *J. Mater. Chem. A*, 2018, **6**, 18669; (*d*) Y. Li, C. Qi, S. Li, H. Zhang, C. Sun, Y. Yu, S. Pang, *J. Am. Chem. Soc.*, 2010, **132**, 12172; (*e*) Y. Xu, L. Tian, D. Li, P. Wang and M. Lu, *J. Mater. Chem. A*, 2019, DOI: 10.1039/C9TA01077g.

3 (*a*) H. Gao and J. M. Shreeve, *Chem. Rev.*, 2011, **111**, 7377; (*b*) Q. Sun, C. Shen, X. Li, Q. Lin and M. Lu, *J. Mater. Chem. A*, 2017, **5**, 11063; (*c*) Z. Xu, G. Cheng, S. Zhu, Q. Lin and H. Yang, *J. Mater. Chem. A*, 2018, **6**, 2239.

4 Y. Tang, H. Gao, L. A. Mitchell, D. A. Parrish and J. M. Shreeve, *Angew. Chem., Int. Ed.*, 2016, **55**, 1147-1150.

5 (*a*) T. M. Klapötke, N. Mayr, J. Stierstorfer and M. Weyrauther, *Chem. –Eur. J.*, 2014, **20**, 1410; (*b*) Y. Tang, J. Zhang, L. A. Mitchell, D. A. Parrish and J. M. Shreeve, *J. Am. Chem. Soc.*, 2015, **137**, 15984; (*c*) Y. Tang, C. He, L. A. Mitchell, D. A. Parrish and J. M. Shreeve, *J. Mater. Chem. A*, 2015, **3**, 23143.

6 H. Huang, Y. Li, J. Yang, R. Pan and X. Lin, *New J. Chem.*, 2017, **41**, 7697.

7 Y. Tang, S. Dharavath, G. H. Imler, D. A. Parrish and J. M. Shreeve, *Chem. –Eur. J.*, 2017, **23**, 9185.

8 C. He, G. H. Imler, D. A. Parrish and J. M. Shreeve, *J. Mater. Chem. A*, 2018, **6**, 16833.

9 A. I. Stepanov, V. S. Sannikov, D. V. Dashko, A. G. Roslyakov, A. A. Astrat'ev and E. V. Stepanova, *Chem. Heterocycl. Compd.*, 2015, **51**, 350.

10 Gaussian 03 (Revision E.01): M. J. Frisch, G. W. Trucks, H. B. Schlegel, G. E. Scuseria, M. A. Robb, J. R. Cheeseman, J. A. Montgomery, Jr., T. Vreven, K. N. Kudin, J. C. Burant, J. M. Millam, S. S. Iyengar, J. Tomasi, V. Barone, B. Mennucci, M. Cossi, G. Scalmani, N. Rega, G. A. Petersson, H. Nakatsuji, M. Hada, M. Ehara, K. Toyota, R. Fukuda, J. Hasegawa, M. Ishida, T. Nakajima, Y. Honda, O. Kitao, H. Nakai, M. Klene, X. Li, J. E. Knox, H. P. Hratchian, J. B. Cross, V. Bakken, C. Adamo, J. Jaramillo, R. Gomperts, R. E. Stratmann, O. Yazyev, A. J. Austin, R. Cammi, C. Pomelli, J. W. Ochterski, P. Y. Ayala, K. Morokuma, G. A. Voth, P. Salvador, J. J. Rabuck, K. Raghavachari, J. B. Foesman, J. V. Ortiz, Q. Cui, A. G. Baboul, S. Clifford, J. Cioslowski, B. B. Stefanov, A. Lo. G. Liu, P. Piskorz, I. Komaromi, R. L. Martin, D. J. Fox, T. Keith, M. A. Al-Laham, C. Peng, A. Nanayakkara, M. Challacombe, P. M. W. Gill, B. Johnson, W. Chen, M. Wong, C. Gonzalez, J. A. Pople, Gaussian, Inc, Wallingford CT, 2004.

11 M. Sućeska, Brodarski Institute, Zagreb, Croatia, EXPLO5, Version 6.01, 2013.

12 a) Tests were conducted according to the UN Recommendations on the Transport of Dangerous Goods, Manual of Tests and Criteria, 5th rev. ed., United Nations Publication, New York, 2009; b) 13.4.2 Test 3 (a)(ii) BAM Fallhammer, pp. 75;c) 13.5.1 Test 3 (b)(i): BAM friction apparatus, pp. 104.

13 Y. Wang, Y. Liu, S. Song, Z. Yang, X. Qi, K. Wang, Y. Liu, Q. Zhang, Y. Tian, *Nat. Commun.*, **2018**, *9*, 2444.

14 (*a*) C. Zhang, X. Wang and H. Huang, *J. Am. Chem. Soc.*, 2008, **130**, 8359. (*b*) Y. Ma, A. Zhang, C. Zhang, D. Jiang, Y. Zhu and C. Zhang, *Cryst. Growth Des.*, 2014, **14**, 4703. (*c*) Y. Ma, A. Zhang, X. Xue, D. Jiang, Y. Zhu and C. Zhang, *Cryst. Growth Des.*, 2014, **14**, 6101.

15 T. Lu and F. Chen, *J. Comput. Chem.*, 2012, **33**, 580.

16 M. S. Westwell, M. S. Searle, D. J. Wales and D. H. Williams, *J. Am. Chem. Soc.*, 1995, **117**, 5013.

17 H. Gao, C. Ye, C. M. Piekarski and J. M. Shreeve, *J. Phys. Chem. C*, 2007, **111**, 10718.

18 P. J. Linstrom, W. G. Mallard, Eds., NIST Chemistry WebBook, NIST Standard Reference Database Number 69, June 2005, National Institute of Standards and Technology, Gaithersburg MD, 20899 (http://webbook.nist.gov).

19 Bruker, *APEX3 v2015.5-2*. Bruker AXS Inc., Madison, Wisconsin, USA, 2015.

20 Bruker, *SAINT v8.34A*. Bruker AXS Inc., Madison, Wisconsin, USA, 2013.

21 Bruker, *XPREP v2014/2*. Bruker AXS Inc., Madison, Wisconsin, USA, 2014.

22 Bruker, *SADABS v2014/5*, Bruker AXS Inc., Madison, Wisconsin, USA, 2014.

23 G. M. Sheldrick, *SHELXL-2014/7*. University of Göttingen, Germany, 2014.

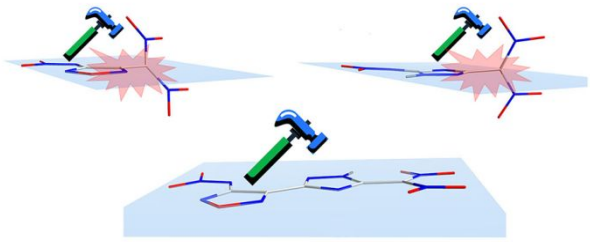

Enlarging the skeleton containing two heterocylic five-membered rings can decrease sensitivity in comparison with most highly nitro-functionalized mono nitrogen-rich rings.